A macrocyclic zinc(II) fluorophore as a detector of apoptosis

Eiichi Kimura*†, Shin Aoki‡, Emiko Kikuta‡, and Tohru Koike‡

*Faculty of Integrated Arts and Sciences, Hiroshima University, Kagamiyama 1-7-1, Higashi–Hiroshima 739-8521, Japan; and ‡Division of Medicinal Chemistry, Graduate School of Biomedical Sciences, Hiroshima University, Kasumi 1-2-3, Minami-ku, Hiroshima 734-8551, Japan

Edited by Kenneth N. Raymond, University of California, Berkeley, CA, and approved January 16, 2003 (received for review November 30, 2002)

Our originally designed dansylamidoethylcyclen 4 as a biomimetic Zn^{2+}-selective fluorophore has been demonstrated to be a good detector of the apoptosis (induced by an anticancer agent, etoposide, and H_2O_2) in cancer cells such as HeLa and HL60 cells. The macrocyclic Zn^{2+} ligand 4 (mostly as a deprotonated form) is cell-permeable to show weak fluorescence (emission at 550 nm), which forms a strong fluorescent 1:1 Zn^{2+} complex 5 (emission at 530 nm) when Zn^{2+} is incorporated into the cells by a zinc(II) ionophore pyrithione. Thus formed, Zn^{2+} complex 5 is cell-impermeable and remains intact over a few hours. When apoptosis in HeLa or HL60 cells is artificially induced, 4 selectively and strongly stains apoptotic cells only at early stages, which was verified by using the conventional apoptosis detection probe annexin V-Cy3. Detection of the apoptotic cells by 4 was perhaps due to significantly increased free Zn^{2+} flux at early stages of apoptosis. Apoptotic detection by 4 has been compared with a presently available Zn^{2+} fluorophore, Zinquin 1. We present that 4 has advantages in detection of apoptosis over annexin V-Cy3 and Zinquin 1.

Apoptosis is a highly programmed cell death mechanism for removal of unwanted cells from tissues and is an important event in tissue development and homeostasis (1–4). Many anticancer agents such as cisplatin (5, 6) and etoposide (7, 8) act by inducing tumor cells to apoptose. Apoptosis is distinguished from necrosis (passive cell death) by a unique series of morphological changes, including a decease in cell volume and budding of the cell contents into membrane-enclosed vesicles. Fragmentation of DNA in apoptotic cells appears on gel electrophoresis (1, 8). Apoptosis is accompanied by a loss of membrane phospholipid asymmetry, resulting in the exposure of phosphatidylserine at the cell surface, which is a principle to be currently used for detection of apoptosis by an annexin V-Cy3 kit (9). Annexin V has a high affinity for phosphatidylserine, whereby the covalently attached fluorescein Cy3 becomes fluorescent (10).

Zinc(II) is now well recognized as an important cofactor in the regulation of apoptosis (11–18). For instance, removal of Zn^{2+} enhances apoptosis, whereas supplementation of Zn^{2+}, whose mechanism is not yet understood, suppresses it (13). Furthermore, intracellular labile zinc(II) flux was observed during apoptosis by using a fluorescent Zn^{2+} probe, Zinquin **1** (for structures of Zn^{2+} ligands, see Fig. 1) (14–18). Zinquin **1** (L^1) is a bidentate ligand, and its hydrolyzed form **2** (L^2) gives 1:1 $[Zn(H_{-1}L^2)]$ and 2:1 $[Zn(H_{-1}L^2)_2]$ complexes **3** with Zn^{2+} in physiological media with a respective stepwise K_d of 3.7×10^{-7} and 8.5×10^{-8} M (14). Metalloproteins have much higher affinities for Zn^{2+}, with K_d typically ranging from 10^{-12} to 10^{-13} M, than does Zinquin **1**. Cellular Zinquin **1** fluorescence could thus be increased to the same extent as in apoptotic cells if there were a substantial release of Zn^{2+} from metalloproteins. It is not clear yet whether the changes in free Zn^{2+} are a cause or a consequence of apoptosis. Zalewski *et al.* (15) hypothesized that the release of Zn^{2+} from the endonuclease early in apoptosis may facilitate DNA fragmentation; i.e., the changes in intracellular Zn^{2+} may be a cause of apoptosis.

A few years ago, while pursuing a model study of carbonic anhydrase, we synthesized a highly efficient macrocyclic Zn^{2+}-selective fluorescent probe **4** (L^3) (18–25). The structure was originally designed as a biomimetic model of the catalytic Zn^{2+} center of carbonic anhydrase that strongly and selectively binds to dansylamide. Characteristic of our probe dansylamidoethylcyclen **4** was its affinity to Zn^{2+} ($K_d = 1.4 \times 10^{-10}$ M at pH 7.0 and 5.5×10^{-13} M at pH 7.8), which was much higher than that of Zinquin **1** (19). The K_d values for the 1:1 Zn^{2+}–**4** complex, **5** $[Zn(H_{-1}L^3)]$ significantly vary at near neutral pH because of the competing protonation. Interestingly, the K_d value of 5.5×10^{-13} M at a pH of 7.8 is comparable to the K_d values for zinc(II) enzymes and the K_d value of 5.7×10^{-12} M at pH 7–7.8 for zinc(II) finger peptides (26, 27). The dansylamide deprotonation in the Zn^{2+} complex **5** at pH 7.8 increased the emission intensity by 4.8-fold at 540 nm and by 10-fold at 490 nm, whereas the nonmetallated dansylamide deprotonation of L to $H_{-1}L^3$ without Zn^{2+} at high pH (>12) brought about only a 20% increase in the fluorescence emission intensity (19). The second-order reaction rate of **4** with Zn^{2+} at neutral pH is 1.7×10^2 $M^{-1}{\cdot}s^{-1}$ (19), which is not as fast as **1**. Until now, there have been few cell-permeable Zn^{2+} fluorophores in the literature (28–31). Zinpyr-1 **6**, for example, was reported by Lippard and coworkers (28, 29); however, its applications may be limited due to its only two to three times increase in quantum yield on Zn^{2+} binding.

In the present study, we have investigated whether this type of Zn^{2+} fluorophore **4** is biologically useful, i.e., cell-permeable, and, if so, what are its special properties in comparison to currently available but weakly Zn^{2+}-binding agents such as Zinquin **1** in detecting intracellular Zn^{2+} flux. We have discovered that among those Zn^{2+} probes, only **4** was a selective and efficient sensor of apoptosis in cancer cells. For the present study, we also have compared **4** with homologous Zn^{2+} fluorophores **7** (19) and **8** (31). Comparison has also been made with Zinquin **1** and commercial apoptosis detection kit annexin V-Cy3 that adopts an entirely different mechanistic principle.

Materials and Methods

All aqueous solutions were prepared by using trace Zn^{2+}-free deionized and redistilled water. A **4** like $L^3{\cdot}(HCl)_5$, either synthesized (19) or purchased from Dojin Kagaku (Kumamoto, Japan), was dissolved in an aqueous buffer solution. Zinquin **1** was a kind gift from P. D. Zalewski (University of Adelaide, Adelaide, Australia), which was stored at 5 mM in dimethyl sulfoxide at −20°C. An *N*-dansyl-*N*,*N*-dimethylethyl-

This paper was submitted directly (Track II) to the PNAS office.

Abbreviations: pyrithione, 2-mercaptopyridine *N*-oxide; TPEN, *N*,*N*,*N*′,*N*′-tetrakis(2-pyridylmethyl)ethylenediamine; PI, propidium iodide.

†To whom correspondence should be addressed. E-mail: ekimura@hiroshima-u.ac.jp.

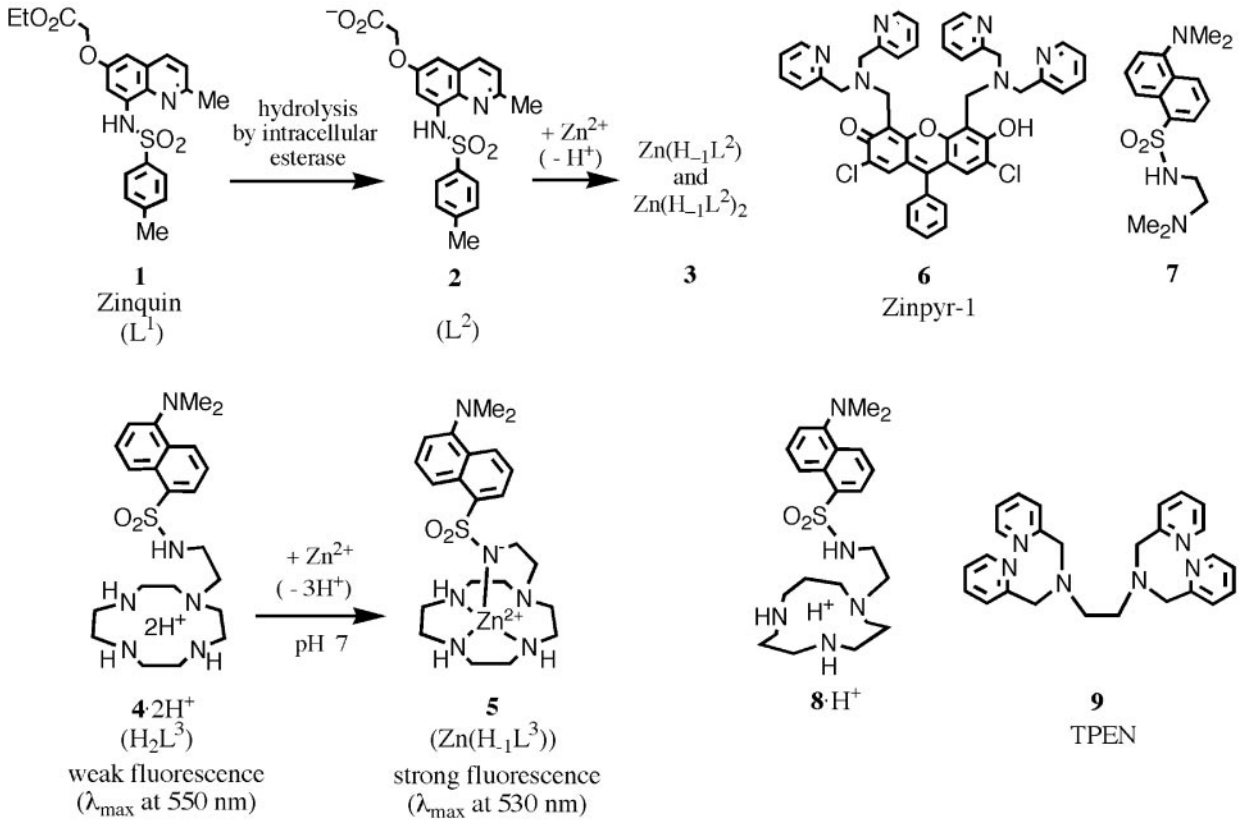

Fig. 1. The structures of zinc(II) fluorophores and zinc(II) chelators used in this study.

enediamine **7** (19) and a dansylamidoethyl-[12]aneN$_3$ **8** (31) were prepared as described. *N*,*N*,*N*′*N*′-tetrakis(2-pyridylmethyl)ethylenediamine (TPEN) **9** was purchased from Sigma.

Preparation of Cultured Cells. Cultured HeLa and HL60 cells were obtained from Cell Resource Center for Biomedical Research, Tohoku University (Sendai, Japan) and were maintained in DMEM (Nissui Seiyaku, Tokyo) supplemented with 10% FBS (GIBCO/BRL)/100 μg/ml streptomycin/100 units/ml penicillin. Cell viability was monitored by trypan blue or propidium iodide (PI) exclusion and phase-contrast microscopy. PI and trypan blue were added to final concentrations of 30 μM and 0.1% (wt/vol), respectively.

Treatment of Cells with Zn^{2+} Ionophores. Cells (5×10^6 per ml) were treated for indicated periods of time at 37°C with 25 μM $ZnSO_4$ (approximate concentration of Zn^{2+} in human plasma is 15 μM) and Zn^{2+} ionophore sodium pyrithione (14–16) in Hanks' balanced salt solution (HBSS). Cells were then washed three times with HBSS to remove extracellular Zn^{2+} before labeling with Zn^{2+} fluorophores **1**, **4**, **7**, and **8**.

Cell Staining. Cells (10^5/100 μl in complete medium) were placed into each well of a 96-well plate. After 24 h, the medium was exchanged for serum-free medium containing a dye, which was then incubated for 30 min. After washing the cells with PBS, observations were made with an Olympus (New Hyde Park, NY) fluorescence microscope. Excitation light was provided by a 150-W Xe arc lamp transmitted through a 400-nm emission filter (Olympus U-MWU cube). Intracellular acidic compartments were visualized by staining with the acridine orange. Excitation light transmitted through a 460- to 490-nm excitation filter and fluorescence was observed after passage through a 500-nm emission filter (Olympus CX-DMB-2 cube).

Fluorescence Microscopy. For measurements of intracellular fluorescence wavelength of Zn^{2+} fluorophores, **1**, **4**, **7**, and **8**, suspended HeLa cells (10^7 cells per ml in medium) or HL60 cells (10^6 cells per ml in medium) were incubated with **1**, **4**, **7**, or **8** (50 μM) for 30 min at 37°C, and cells were washed three times with PBS buffer, then suspended in PBS in cuvettes. For measurement of intracellular Zn^{2+} complex of **1** or **4**, cells incubated with **1** or **4** were treated with 25 μM $ZnSO_4$ and 20 μM pyrithione for 10 min at 37°C in medium and washed three times with PBS buffer. Fluorescence of cell suspension was measured at 25 ± 0.1°C in a Hitachi (Tokyo) 4500 fluorescence spectrophotometer at excitation wavelength of 330 nm.

Results and Discussion

Intracellular Staining with 4. Incubation of cells with 50 μM **4** for 1 h produced all bright punctate staining patterns similar to observations made with Zinquin **1** (14, 15) and Zinpyr-1 **6** (28, 29). The brightly fluorescing cells by **4** were seen in cultured cell populations tested, including human cervix epitheloid carcinoma HeLa cells and human promyelocytic leukemia HL60 cells. It is to be noted that **4** (100 μM) by itself induced apoptosis on exposure over 48 h. However, a short exposure (e.g., 1 h) did not cause significant damage to HeLa cells. Fig. 2*A* shows intensely fluorescent HeLa cells stained with 50 μM **4**. A significant enhancement of the blue-shifted fluorescence in the puncta could be observed when the cells were exogeneously treated for 15 min with a mixture of Zn^{2+} (25 μM) and zinc(II) ionophore pyrithione (2-mercaptopyri-

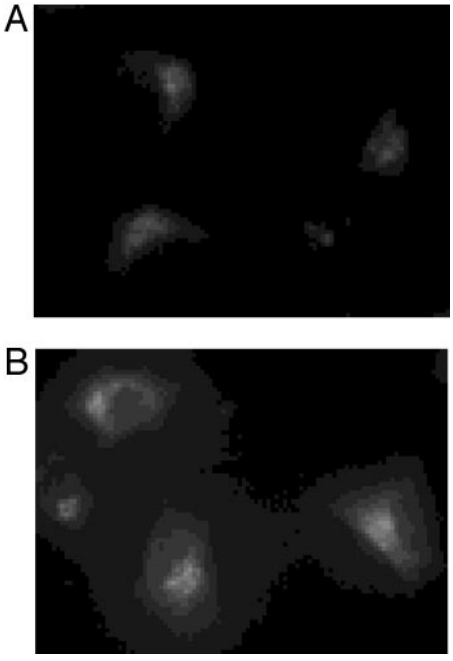

Fig. 2. (*A*) Fluorescence microscopy images (×400) of HeLa cells labeled with 50 μM **4** for 1 h at 37°C, and the fluorescence emission maximum at 550 nm, indicating that fluorescence is not Zn^{2+}-induced. (*B*) The bright perinuclear punctate staining (emission maxima at 530 nm) increases on addition of the zinc(II) ionophore, Zn^{2+}–pyrithione, indicating the intracellular Zn^{2+}– **4** complexation (to yield **5**).

dine *N*-oxide, 20 μM) (Fig. 2*B*). Acridine orange tends to be trapped (as red fluorescence) in acidic compartments of cells as a membrane-impermeable protonated species, due to its weak acidity (pK_a = 9.8). **4** also stained the same acidic compartments of cells, due to similar weak acidities (pK_a = 11.8, 10.8, 9.37, and 4.03). Namely, a less protonated **4** permeates the cellular membrane, but on more protonations in the acidic cell compartment, **4** would be impermeable and remain emitting weak fluorescence (at 550 nm). The initial fluorescence of Zn^{2+}–**4** complex **5** was not readily diminished by addition of a far stronger Zn^{2+}-chelator, TPEN **9** [K_d for Zn^{2+}-TPEN is 6.3×10^{-16} M at pH 7.6 (32)], probably due to kinetic inertness of the macrocyclic Zn^{2+} complex **5**. The strong intracellular fluorescence from **5** remained intact over several hours. Separately, we found that the fluorescence of **5** hardly disappeared by addition of TPEN in a test tube. For comparison, Zinquin **1** by itself (25 μM, the predetermined optimal concentration) stained HeLa cells only a little, but it emitted strong blue-fluorescence when contacted with zinc(II)-pyrithione. However, the intracellular fluorescence by the Zn^{2+}–Zinquin complexes **3** did not last so long as originally reported of chronic lymphocytic leukemia cells by Zalewski *et al*. (15); i.e., within 10–20 sec, the fluorescence from **3** in HeLa cells became quenched. It is to be emphasized that unlike Zinquin complexes **3**, the Zn^{2+}– **4** complex **5** was much more stable kinetically, thermodynamically, and toward UV light. In comparison to cell-permeable Zinpyr-1 **6** reported by Lippard *et al*., whose fluorescence was strongly enhanced not only by Zn^{2+} but also by protonation (especially at neutral pH), our **4** obviously has more advantage. Another advantage was that metal-free **4** having weak emission maximum at 550 nm is distinguished from the Zn^{2+}–bound **4** having blue-shifted fluorescence at 530 nm. It is now concluded that the free ligand **4** as a protonated form (H_2L^3) is outer-membrane-permeable at neutral pH and forms a thermodynamically and kinetically stable 1:1 Zn^{2+} complex **5** emitting stronger blue-shifted fluorescence. The complex **5** remained impermeable and did not diffuse for a long period. Because the nucleic acid and membrane bleb were devoid of the **4**-derived fluorescence, we concluded that **4** would localize only in extranuclei cytoplasm.

After we learned that our zinc(II) fluorophore **4** appeared useful in detecting intracellular Zn^{2+} influx, we have tested **4** to see how it may image apoptotic processes in cancer cells that may or may not involve the intracellular zinc(II) flux.

Apoptotic Morphology of HeLa Cells. The HeLa cells were incubated with an anticancer agent etoposide (100 μM, 48 h, 37°C) to induce apoptosis (7, 8). The earliest morphological change occurred to cell size. At 48 h, a subpopulation of cells demonstrated marked shrinkage (36 ± 6%). At longer time periods, all of the dying cells shrank. As another indication of apoptosis, internucleosomal digestion of DNA occurs at an early event of apoptosis (before cell shrinkage). Etoposide broke DNA in 48 h after incubation, as shown by 180-bp DNA ladders on gel electrophoresis (data not shown). The apoptosis-induced HeLa cells (stained with **4**) were examined simultaneously by phase-contrast and UV fluorescence microscopy. Very brightly fluorescent apoptotic cells were discernible from nonfluorescent viable (intact) cells. The morphological features of apoptosis include membrane blebbing, decrease in cell volume, and pyknotic nuclei in the phase-contrast microscopic image. Although shrunken apoptotic cells were brightly fluorescent, there was no simple correlation between degree of shrinkage and fluorescence intensity. Another apoptosis-inducing agent, H_2O_2 (0≈1 mM; ref. 33), also increased proportion of Zn^{2+}-rich cells with similar apoptotic morphological changes.

Dual Labeling of Apoptotic HeLa Cells with 4 and Vital Dye PI. Viable cells seen by phase-contrast microscopic image were devoid of fluorescence. At early stages of apoptosis (for example, treatment with etoposide for at 6 h; Fig. 3 *A* and *B*), brightly fluorescent apoptotic cells emerged, but these apoptotic cells still excluded the vital dye PI (Fig. 3 *C* and *D*), indicating that an increase in the fluorescence by **4** preceded changes in inner membrane permeability. Later in the etoposide culture (for example, at 48 h), however, the later stages of apoptotic cells permitted the inner membrane permeability of the vital dye PI to allow pink-red-colored fluorescence emission (620 nm) from the nucleus DNA-bound PI (Fig. 3 *G*–*J*).

By contrast, cell necrosis induced by a high concentration (80 mM) of H_2O_2 (33) was not accompanied by an increase in fluorescence from **4**; rather, the fluorescence diminished to almost none. Furthermore, these dead cells lacked the morphological features of apoptosis. The inner membranes were leaky of the vital dye PI to permit red florescent interaction with DNA and did not contain fragmented DNA (data not shown).

Intracellular Staining with Other Relevant Zn^{2+} Fluorophores. To check that the brighter fluorescence by **4** in HeLa apoptosis was due to increased release in Zn^{2+}, we first tried to stain HeLa cells with homologues **7** or **8** (100 μM, 30 min, 37°C) that were shown to bind with Zn^{2+} as less strongly as **4** (19, 31). We saw that **7** and **8** similarly permeated the outer membrane to weakly fluoresce with similar perinuclear punctate staining pattern, as seen with **4** (Fig. 4*A*). However, when **7**- (or **8**)-permeated cells were treated with various concentrations of Zn^{2+} (10–100 μM)–pyrithione (8–80 μM), the fluorescence intensity did not change (Fig. 4*B*), indicating that **7** and **8** could not detect cellular Zn^{2+}. We also observed that

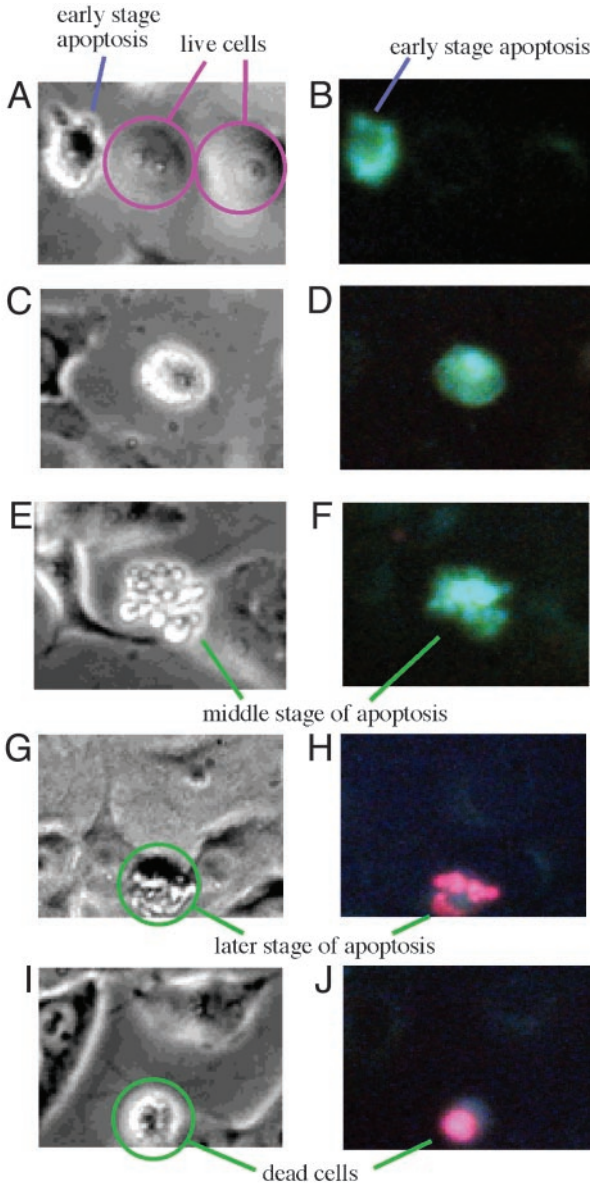

Fig. 3. Morphological changes of HeLa cells (dually labeled with **4** and PI) by simultaneous phase contrast (*A*, *C*, *E*, *G*, and *I*) and fluorescence (*B*, *D*, *F*, *H*, and *J*) microscopy (×400). (*A* and *B*) Live cells and the early stages of apoptotic cells. (*C* and *D*) Early stage of apoptosis. (*E* and *F*) Middle stages of apoptosis. (*G* and *H*) Later stages of apoptosis. (*I* and *J*) Dead cells.

on staining apoptotic HeLa cells [with etoposide (100 μM) cultured for 48 h] with **7** or **8**, the intracellular fluorescences did not intensify, as observed with **4**.

To further test that the brighter fluorescence of **4** in apoptotic cells was due to the flux of free Zn^{2+}, we examined the effect of the stronger Zn^{2+} chelator TPEN **9**, which acts as an intracellular Zn^{2+} ligand (13–18). Apoptosis-induced HeLa cells were treated with TPEN (100 μM) for 2 h after staining with **4** or Zinquin **1**. TPEN did not so clearly eliminate the bright fluorescence of **4** as the bright fluorescence of **1**. Therefore, it may not be conclusive that the enhanced fluorescence of **4** in apoptosis was due to increased Zn^{2+}. However, we could explain this result by the fact that the intracellular ligand displacement of macrocyclic complex **5** by TPEN was kinetically too slow. Although we tentatively postulated that the brighter fluorescence of **4** in apoptotic cells is due to

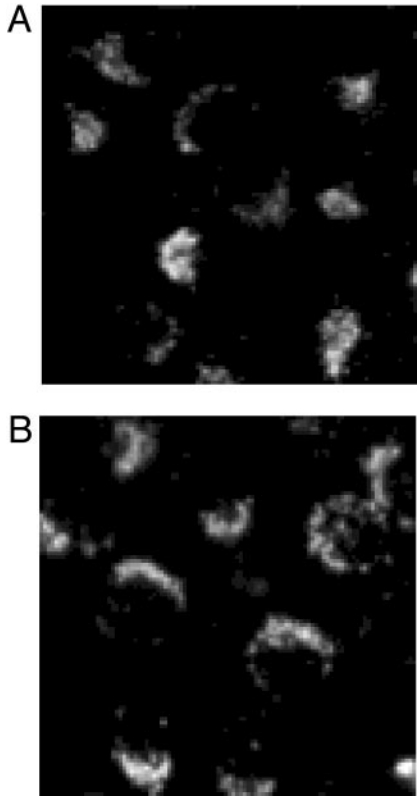

Fig. 4. **7** (100 μM)-loaded HeLa cells with UV fluorescence. Images are from before (*A*) and after (*B*) increasing intracellular Zn^{2+} concentration using sodium pyrithione.

increased Zn^{2+} flux, another mechanism, such as altered behaviors of probe **4** to permeate apoptotic cells, may not be completely excluded in accounting for the brighter fluorescence.

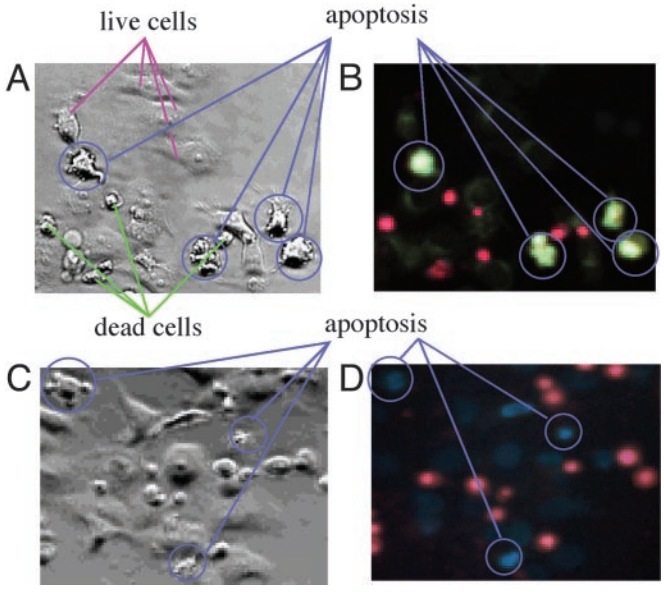

Fig. 5. Comparison of microscopic images (×400) of apoptosis by **4** [*A* (phase contrast) and *B* (fluorescence)] and by Zinquin 1 [*C* (phase contrast) and *D* (fluorescence)]. Etoposide (100 μM, 48 h)-treated HeLa cells were dually stained with **4** (100 μM) or Zinquin **1** (50 μM) and PI (30 μM). Both fluorophores were excited at 330–350 nm.

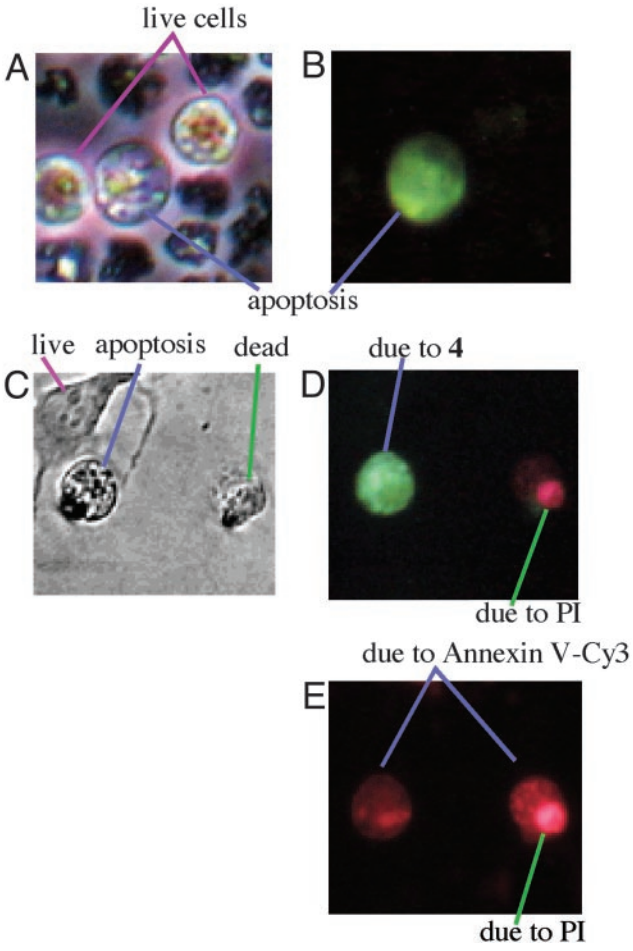

Fig. 6. Phase-contrast (*A*) and fluorescent (*B*) images (×400) of apoptotic HL60 cells stained with **4**. (*C–E*) Phase-contrast image (*C*), fluorescent image [irradiated with UV (330–350 nm), *D*], and fluorescent image [irradiated with visible light (460–490 nm), *E*] of apoptotic HeLa cells triply stained with **4**, annexin V-Cy3, and PI, showing green-fluorescent apoptotic cells by **4** (*D*), and red-fluorescent apoptotic cells by annexin V-Cy3 (*E*) with red-fluorescent dead cells by PI.

Comparison of Fluorescence Microscopic Images of Apoptosis by 4 and Zinquin 1. For practical apoptotic detection, we have compared our new probe **4** (100 μM, 1 h) (Fig. 5*A*) with Zinquin **1** (50 μM, 1 h) (Fig. 5*B*) on HeLa cells apoptosis in the presence of PI. With either Zn^{2+} fluorophore, the simultaneous phase contrast and fluorescence microscopic pictures gave similar detection of intact (live) cells by weak fluorescences, apoptotic cells by brighter fluorescences, and the PI-stained necrotic or dead cells. Furthermore, we found that the brighter fluorescence by **4** was stable and sustained more than several hours, whereas the brighter fluorescence by Zinquin **1** disappeared in 10–20 sec. These results demonstrate that our macrocyclic probe **4** is another useful apoptotic detection probe. Statistic determination of apoptotic HeLa cells by **1** or **4** was preliminarily attempted at several concentrations of etoposide (see Fig. 7, which is published as supporting information on the PNAS web site, www.pnas.org). However, we have failed so far to obtain quantitative results.

Fluorescence Microscopic Image of Apoptotic HL60 Cells by 4. The remarkable increase in fluorescence emission of **4** was also observed with another kind of cancer HL60 cells in apoptosis induced by etoposide (100 μM, 48 h). The phase-contrast and fluorescence microscopic pictures (Fig. 6 *A* and *B*) clearly distinguished brighter green-fluorescent apoptotic cells from very weak fluorescent intact (live) cells and nonfluorescent dead cells, a fact that enhances a potential usefulness of **4** as an apoptosis probe. Separately, we confirmed the apoptotic HL60 cells by the after annexin V-Cy3 detector.

Triply Stained Apoptotic HeLa Cells with 4, Annexin V-Cy3, and PI. The present apoptosis detection by **4** has been compared with a currently available annexin V-Cy3 method (9), which adopts an totally different chemical principle. Entry into apoptosis or necrosis leads to a loss of phospholipid asymmetry with exposure of phosphatidylserine on the outer leaflet. The anticoagulant annexin V binds to the negatively charged phosphatidylserine on the membrane of apoptotic cells as well as dead cells. Fluorescein isothiocynate (Cy3)-labeled annexin V thus stains apoptotic and dead cells. The binding of annexin V correlates with apoptotic nuclear morphology and DNA fragmentation (10). To compare our probe **4** with annexin V for staining apoptotic cells, apoptotic HeLa cells cultured as described above were triply stained with **4**, annexin V-Cy3, and PI for 1 h at 37°C. Fig. 6*C* shows phase-contrast microscopic images of viable (live), apoptotic, and dead cells as morphologically distinguished. Irradiation with UV light (330–350 nm) showed only the apoptotic cells with intensely green fluorescence from **4** (Fig. 6*D*). The same apoptotic cells also have been stained by annexin V-Cy3 (Fig. 6*E*), as shown by red fluorescence [irradiated with visible light (460–490 nm)]. These findings are another proof that **3** is as good as the conventional annexin V probe in detecting apoptosis. Moreover, the annexin V-Cy3 method requires the double stain together with PI to distinguish apoptosis from necrosis (9, 10), because annexin V also binds to dead cells. PI distinguishes dead cells from apoptotic cells. As an advantage, our probe **4** acts alone to distinguish apoptosis from necrosis.

Conclusion

First, we found a Zn^{2+} fluorophore **4** to be a useful biological Zn^{2+} probe. **4** may be useful for quantification of Zn^{2+} concentrations in zinc(II)-rich cells including secretory cells or inflammatory cells (34). Secondly, we have demonstrated that **4** may be a new and more practical detector of apoptosis than previously reported Zinquin **1** or annexin V-Cy3 probes. The comparable Zn^{2+}-affinities of **4**, Zn^{2+} enzymes, and Zn^{2+} finger proteins may be helpful in examining the mechanism of Zn^{2+} flux in the apoptotic processes.

S.A. thanks the Uehara Memorial Foundation (Tokyo), the Asahi Glass Foundation (Tokyo), and the Research Foundation for Pharmaceutical Sciences (Tokyo), and S.A. and E. Kikuta thank the Takeda Science Foundation (Osaka). This work was supported by Ministry of Education, Science, and Culture, Japan Grants 08249103 and 12470479 (to E. Kimura), and 12033237, 12771355, and 13557195 (to S.A.).

1. Lavin, M. & Watters, D. (1993) *Programmed Cell Death: The Cellular and Molecular Biology of Apoptosis* (Harwood, Melbourne).
2. Vaux, D. J. & Korsmeyer, S. J. (1999) *Cell* **96,** 245–254.
3. Evans, G. I. & Vousden, K. H. (2001) *Nature* **411,** 342–348.
4. Huang, Z. (2002) *Chem. Biol.* **9,** 1059–1072.
5. Barry, M. A., Behnke, C. A. & Eastman, A. (1990) *Biochem. Pharmacol.* **40,** 2353–2362.
6. Ishibashi, T. & Lippard, S. J. (1998) *Proc. Natl. Acad. Sci. USA* **95,** 4219–4223.
7. Shimizu, T., Kubota, M., Tanizawa, A., Sano, H., Kasai, Y., Hashimoto, H., Akiyama, Y. & Mikawa, Y. (1990) *Biochem. Biophys. Res. Commun.* **169,** 1172–1177.
8. Forbes, I. J., Zalewski, P. D., Giannakis, C. & Cowled, P. A. (1992) *Exp. Cell Res.* **198,** 367–372.

9. Vermes, I., Haanen, C., Steffens-Nakken H. & Reutelingsperger, C. (1995) *J. Immunol. Methods* **184,** 39–51.
10. Koopman, G., Reutelingsperger, C. P. M., Kujiten, G. A. M., Keehnen, R. M. J., Pals, S. T. & van Oers, M. H. J. (1994) *Blood* **84,** 1415–1420.
11. Treves, S., Trentini, P. L., Ascanelli, M., Bucci, G. & Di Virglio, F. (1994) *Exp. Cell. Biol.* **211,** 339–343.
12. Cuajungco, M. P. & Lees, G. J. (1997) *Neurobiol. Dis.* **4,** 137–169.
13. Truong-Tran, A. Q., Carter, J., Ruffin, R. E. & Zalewski, P. D. (2001) *BioMetals* **14,** 315–330.
14. Zalewski, P. D., Forbes, I. J. & Betts, W. H. (1993) *Biochem. J.* **296,** 403–408.
15. Zalewski, P. D., Forbes, I. J., Seamark, R. F., Borlinghaus, R., Betts, W. H., Lincoln, S. F. & Ward, A. D. (1994) *Chem. Biol.* **1,** 153–161.
16. Zalewski, P. D., Millard, S. H., Forbes, I. J., Kapaniris, O., Slavotinek, A., Betts, W. H., Ward, A. D., Lincoln, S. F. & Mahadevan, I. (1994) *J. Histochem. Cytochem.* **42,** 877–884.
17. Sarwar Nasir, M., Fahrni, C. J., Suhy, D. A., Kolodsick, K. J., Singer, C. P. & O'Halloran, T. V. (1999) *J. Biol. Inorg. Chem.* **4,** 775–783.
18. Fahrni, C. J. & O'Halloran, T. V. (1999) *J. Am. Chem. Soc.* **121,** 11448–11458.
19. Koike, T., Watanabe, T., Aoki, S., Kimura, E. & Shiro, M. (1996) *J. Am. Chem. Soc.* **118,** 12696–12703.
20. Kimura, E. (1997) *S. Afr. J. Chem.* **40,** 240–248.
21. Kimura, E. & Koike, T. (1998) *Chem. Soc. Rev.* **27,** 179–184.
22. Kimura, E. & Koike, T. (1998) *J. Chem. Soc. Chem. Commun.* 1495–1500.
23. Kimura, E. & Kikuta, E. (2000) *J. Biol. Inorg. Chem.* **5,** 139–155.
24. Kimura, E. & Aoki, S. (2001) *BioMetals* **14,** 191–204.
25. Aoki, S., Kaido, S., Fujioka, H. & Kimura, E. (2003) *Inorg. Chem.* **43,** 1023–1030.
26. Krizek, B. A., Merkle, D. L. & Berg, J. M. (1993) *Inorg. Chem.* **32,** 937–940.
27. Lippard, S. J. & Berg, J. M. (1994) *Principles of Bioinorganic Chemistry* (University Science Books, Mill Valley, CA)
28. Walkup, G. K., Burdette, S. C., Lippard, S. J. & Tsien, R. Y. (2000) *J. Am. Chem. Soc.* **122,** 5644–5645.
29. Burdette, S. C., Walkup, G. K., Springer, B., Tsien, R. Y. & Lippard, S. J. (2001) *J. Am. Chem. Soc.* **123,** 7831–7841.
30. Maruyama, S., Kikuchi, K., Hirano, T., Urano, Y. & Nagano, T. (2002) *J. Am. Chem. Soc.* **124,** 10650–10651.
31. Koike, T., Abe, T., Takahashi, K., Ohtani, K., Kimura, E. & Shiro, M. (2002) *J. Chem. Soc. Dalton Trans.* 1764–1768.
32. Outten, C. E. & O'Halloran, T. V. (2001) *Science* **292,** 2488–2492.
33. Ikeda, K., Kajiwara, K., Tanabe, E., Tokumaru, S., Kishida, E., Masuzawa, Y. & Kojo, S. (1999) *Biochem. Pharmacol.* **57,** 1361–1365.
34. Frederickson, C. J. (1989) *Int. Rev. Neurobiol.* **31,** 145–238.